Vorbeck, M. L., and Marinetti, G. V. (1965), *J. Lipid Res. 6*, 3.
Ward, J. B., and Perkins, H. R. (1968), *Biochem. J. 106*, 391.
Wieland, O. (1963), *in* Methods of Enzymatic Analysis, Bergmeyer, H. U., Ed., New York, N. Y., Academic Press, p 22.
Yamakawa, T., Irie, R., and Iwanage, M. (1960), *J. Biochem. (Tokyo) 48*, 490.
Yamakawa, T., and Ueta, N. (1964), *Jap. J. Exp. Med. 34*, 37.
Yoshida, M. (1972), *Biochemistry 11*, 1087.
Yoshida, M., and Oshima, T. (1971), *Biochem. Biophys. Res. Commun. 45*, 495.
Yoshizaki, F., Oshima, T., and Imahori, K. (1971), *J. Biochem. (Tokyo) 69*, 1083.

A Comparison of the Kinetics and Stoichiometry of Proton Uptake with Aldehyde Reduction for Liver Alcohol Dehydrogenase under Single Turnover Conditions†

Michael F. Dunn

ABSTRACT: The equine liver alcohol dehydrogenase catalyzed reduction of aldehydes by reduced nicotinamide adenine dinucleotide (NADH) involves the uptake of 1 mol of hydrogen ion/mol of aldehyde reduced (*e.g.*, aldehyde + NADH + $H^+ \rightleftharpoons$ alcohol + NAD^+). A rapid-mixing kinetic technique utilizing a pH indicator–buffer system has been employed in this study to investigate the relationship of proton uptake to the chemical steps involved in the catalytic mechanism. Our previous studies (Bernhard, S. A., Dunn, M. F., Luisi, P. L., and Schack, P. (1970), *Biochemistry 9*, 185) have shown that reduction of aromatic aldehydes in the pH region 8–10 occurs *via* two kinetic processes, a "burst" and a slow step, each of equal concentration change under conditions of excess enzyme. These two processes are remarkably different in rate at pH 8.8 (~200 sec^{-1} and 0.2–10 sec^{-1}, depending on the substrate). Each step involves a net conversion of reactants to products in approximately equal amounts under these single-turnover conditions. In this study, it has been found that under single-turnover conditions the *total* change in hydrogen ion concentration predicted by the chemical reaction occurs in a single first-order process with a rate identical with the rate of the slow step. *No net uptake of protons from solution occurs in the burst process* even though one-half of the net transformation occurs in this step. In a control kinetic study it was found that the displacement of enzyme-bound NAD^+ by NADH is accompanied by the uptake of hydrogen ion from solution by the enzyme. It is proposed that this phenomenon has its origins in a coenzyme oxidation-state-dependent perturbation of the pK_a' of an enzyme-site residue. It also is proposed that the pK_a' perturbation (a) accounts for the absence of a burst uptake of protons during the burst reduction of aldehyde, and (b) is linked to the manifestation of catalytic nonequivalence of the two enzyme catalytic sites.

In our previous studies we have used the stopped-flow, rapid mixing kinetic technique to investigate transient kinetic steps in the horse liver alcohol dehydrogenase (hereafter simply called alcohol dehydrogenase) catalyzed reduction of chromophoric aromatic aldehydes and an aldehyde analog (Bernhard *et al.*, 1970; Dunn and Bernhard, 1971). These studies have shown that reduction occurs in two distinct kinetic steps when the reaction is limited to a single turnover of enzyme sites. Each step corresponds to the net conversion of reactants to products in approximately equal amounts. When NADH[1] and aldehyde are present in large excess of the site concentration, there is a presteady-state burst conversion of reactants to products in an amount equal to one-half of the total site concentration. On the strength of these findings, we concluded that the two alcohol dehydrogenase sites become catalytically nonequivalent during a single-turnover cycle. Additional kinetic evidence in support of this interpretation has been reported by McFarland and Bernhard (1972) and by Luisi and Favilla (1972); and Everse (1973) has reported equilibrium binding studies consistent with this view.

Both the amino acid sequence (Jörnvall, 1973) and the low-resolution X-ray structure work (Brändén *et al.*, 1973) indicate that the crystalline native enzyme is composed of two identical subunits. The crystalline native enzyme exhibits orthorhombic symmetry (space group $C222_1$) with a crystallographic twofold axis of symmetry through the dimeric molecule. The crystalline enzyme–coenzyme complex exhibits a lower crystal symmetry (Brändén *et al.*, 1973). The symmetry loss on complex formation is believed to reflect a loss of symmetry at the molecular level.

The present work examines the relationship between the two-step process for the reduction of 4-(2′-imidazolylazo)-benzaldehyde (azoaldehyde, I) and the process of hydrogen

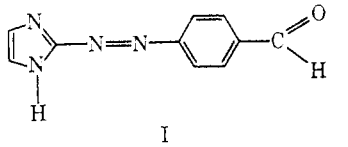

I

ion uptake (eq 1) from solution under single-turnover condi-

$$R{-}\overset{O}{\overset{\|}{C}}{-}H + NADH + H^+ \overset{E}{\rightleftharpoons} R{-}CH_2OH + NAD^+ \quad (1)$$

† From the Department of Biochemistry, University of California, Riverside, California 92502. *Received October 12, 1973.* This work was supported by Grant No. GB-31151 from the National Science Foundation.

[1] Abbreviations used are: NADH and NAD^+, reduced and oxidized nicotinamide adenine dinucleotide, respectively; azoaldehyde and azoalcohol, 4-(2′-imidazolylazo)benzaldehyde and 4-(2′-imidazolylazo)-benzyl alcohol, respectively.

tions at pH 8.8. Note that the stoichiometry of eq 1 requires the uptake of 1 mol equiv of hydrogen ion/mol of aldehyde reduced.

The results of these stopped-flow kinetic studies show that, under single-turnover conditions, the stoichiometrically required amount of hydrogen ion uptake occurs at a rate which is identical to the rate of the slower, second step, and that there is no change in hydrogen ion concentration during the burst reaction. The relationship of these findings to the functioning of the two alcohol dehydrogenase catalytic sites is discussed, and a mechanism for the two-step sequence is proposed.

Materials and Methods

Materials. Water-soluble Thymol Blue (Matheson, Coleman and Bell, reagent, ACS grade), NAD^+ (Boehringer Mannheim Corp., grade I or Sigma, grade III), pyrazole (Aldrich), and acetonitrile (Baker Chemical Co., reagent grade) were used without further purification. NADH (Sigma, grade III) was subjected to four cycles of solution and lyophilization in distilled water to remove trace amounts of ethanol. 4-(2-Imidazolylazo)benzaldehyde (azoaldehyde) was prepared as previously described (Bernhard *et al.*, 1970).

Horse liver alcohol dehydrogenase (Boehringer Mannheim Corp.) was further purified in a modification of the method of Bernhard *et al.* (1970). The clear supernatant aqueous Na_2HPO_4–ethanol solution from 100 mg of the commercial preparation was removed and discarded. The residual enzyme slurry was then dissolved in 10 ml of distilled water and 1 ml of 0.1 M sodium pyrophosphate buffer (pH 8.75). An ethanol-free enzyme preparation was obtained by lyophilizing the solution to a powder, followed by solution and lyophilization a second time. The lyophilized material was then dissolved in distilled water (~12.5 mg of E/ml) and incubated for 16–20 hr at 4° with 1,4-dithioerythritol (0.5 mM). Elution of the incubated enzyme over a 3 × 30 cm Bio-Gel P-30 (Bio-Rad, 50–100 mesh) column equilibrated with 0.05 M NaCl (carbonate free) solution at 4° (pH ~6.5) freed the preparation of buffer ions.

The coenzyme binding titer of the resulting alcohol dehydrogenase solution, reported as N the normality of the coenzyme binding sites, was determined as previously described (Theorell and Yonetani, 1963; Bernhard *et al.*, 1970). Site normalities determined in this way account for 80–95% of the amounts predicted by the 280-nm molar extinction coefficient for alcohol dehydrogenase (Dalziel, 1957).

Kinetic Measurements. The stopped-flow rapid-mixing kinetic experiments were carried out using the Durrum Model D-110 stopped-flow spectrophotometer equipped with a 2-cm Kel-F fluorescence–absorption cuvette (mixing dead-time <3 msec) as previously described (Dunn and Hutchison, 1973).

In a typical experiment, enzyme–NADH solutions buffered with Thymol Blue were prepared and adjusted to pH 8.8 ± 0.1 by the careful addition of carbonate-free dilute NaOH from a micrometer syringe. Azoaldehyde solutions buffered with Thymol Blue were adjusted to pH 8.8 ± 0.1 in the same way. After pH adjustment, both solutions were immediately transferred to the stopped-flow apparatus for the herein described kinetic studies.

After mixing in the stopped flow apparatus, the time course of the transmission changes accompanying the transformation of azoaldehyde to azoalcohol were measured at 390 nm ($\Delta\epsilon_{390} = 8.8 \times 10^3$ M^{-1} cm^{-1} OD) a wavelength where the acid–base-mediated Thymol Blue spectral changes are small in comparison. The pH changes accompanying reaction were monitored by measuring the concomitant changes in the spectrum of Thymol Blue at either 590 nm ($\epsilon_{590} = 2.20 \times 10^4$ M^{-1} cm^{-1} OD) or 650 nm ($\epsilon_{650} = 3.4 \times 10^3$ M^{-1} cm^{-1} OD), respectively, for dilute (<0.1 mM) or concentrated (>0.1 mM) indicator concentrations. Transmission changes resulting from pH perturbations brought about by the mixing of Thymol Blue solutions (pH 8.8) with buffer solutions of a different pH in the stopped-flow apparatus to give a significantly different final pH were complete within the mixing dead time. These experiments established that the time course for the establishment of the Thymol Blue ionization equilibria is rapid relative to the stopped-flow mixing dead time (>3 msec).

Rate constants and optical density changes were calculated as previously described (Dunn and Hutchison, 1973). The experimentally determined rate constants are reported respectively as k_{590} and k_{650} for the Thymol Blue changes, and k_{390} for the second (slow) step observed for the azoaldehyde changes (see Results) according to the wavelength of observation. In each instance, the progress curve was found to follow the assumed first order rate law to at least 90% (>3 half-lives) completion.

Steady-state kinetic measurements using dilute (~10^{-8} N) enzyme concentrations at pH 8.80 were carried out as previously described (Bernhard *et al.*, 1970). The rate of azoaldehyde turnover as measured by changes in optical density at 390 nm was found to be unaffected by the presence of Thymol Blue at concentrations below 0.1 mM. Owing to the large optical density background contributed by Thymol Blue, rate measurements at 390 nm could not be made on solutions significantly more concentrated in Thymol Blue.

In other stopped-flow experiments, the 650-nm Thymol Blue spectral changes were used to investigate the kinetic course of the pH changes which accompany the displacement of enzyme-bound NAD^+ by NADH at pH 8.80 ± 0.1 (see Results). In this experiment, Thymol Blue buffered enzyme–NAD^+ solutions were mixed with Thymol Blue buffered NADH solutions in the stopped-flow apparatus. In a separate experiment, the same solutions (minus Thymol Blue) buffered with 0.5 mM sodium pyrophosphate (pH 8.80 ± 0.1) were used to study the rate of formation of the characteristic enzyme–NADH complex by measuring the optical density changes at a wavelength (365 nm, $\Delta\epsilon_{365} = 2.90 \times 10^3$ M^{-1} cm^{-1} OD) near the maximum difference between the spectrum of the complex and the spectrum of NADH free in solution (Taniguchi *et al.*, 1967; Sund and Theorell, 1962). The optical density at 330 nm (the apparent isosbestic point for free and enzyme-bound NADH) was found to be invariant over the time span necessary for completion of the 365-nm optical density changes in these experiments.

Determination of Relative Buffering Capacities. The relative hydrogen ion buffering capacities for the various solution components employed in these experiments were determined by NaOH titration using the Cary Model 401 vibrating reed electrometer with pH attachment and a combination calomel–KCl microelectrode (A. H. Thomas Co.). The electrometer pH readings, to a precision of ±2 × 10^{-4} pH unit, were measured with a Leeds Northrup potentiometer (as a null device) in the circuit as described by Keiser and Bernhard (1966).

Titrations were performed by adding microliter aliquots of dilute sodium hydroxide solution (0.05 M NaCl) from a Gilmont micrometer syringe to a thermostated reaction vessel containing the carbonate-free sample. The buffering capac-

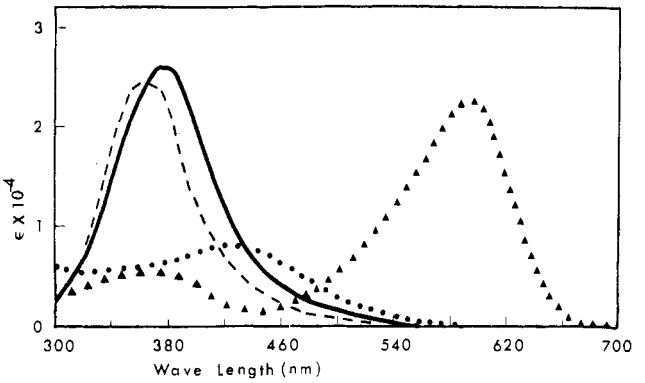

FIGURE 1: Comparison of individual spectra for the azoaldehyde–Thymol Blue system; azoaldehyde (—), azoalcohol (---), Thymol Blue pH 10.87 (▲), Thymol Blue pH 6.00 (●). The spectrum of the azoalcohol was obtained as previously described (Bernhard *et al.*, 1970).

ities of Thymol Blue and of the E–NADH stock solutions employed in the azoaldehyde stopped-flow studies were then calculated at pH 8.80 from the respective plots of millivolts (the potentiometer readings) *vs.* the microliters of added NaOH. The buffering capacities (the reciprocal slope value, μl/mV at the millivolt value corresponding to pH 8.80) were found to be respectively 3.55 and 0.623 for Thymol Blue and the E–NADH stock. Thus, a relative buffering capacity, calculated as $R = (3.55)/(3.55 + 0.623) = 0.85$, was obtained for 6×10^{-4} M Thymol Blue.

The titration plots were calibrated in pH units with reference to the electrode potentials of standard pH solutions.

Determination of ε and pK_a' Values. The pK_a' values for the conjugate acids of the azoaldehyde ($pK_a' = 4.2$) and Thymol Blue ($pK_a' = 8.8$) were determined from the pH dependence of the uv-visible spectrum for each compound by standard methods (Bates, 1964).

Results

Stopped-Flow Studies on the Horse Liver Alcohol Dehydrogenase–Azoaldehyde System. Figure 1 compares the spectrum of Thymol Blue (pH 10.87 and pH 6.00) with the spectrum of azoaldehyde and the spectrum of azoalcohol. At 390 nm, the Δε value for the interconversion of the acidic and basic forms of Thymol Blue ($\Delta\epsilon_{390} = 1.8 \times 10^3$ M^{-1} cm^{-1} OD) is 20% of the Δε value for the conversion of azoaldehyde to azoalcohol ($\Delta\epsilon_{390} = 8.8 \times 10^3$ M^{-1} cm^{-1} OD). Therefore, it was possible to monitor the azoaldehyde transformation at 390 nm in the presence of Thymol Blue, although there is some interference at this wavelength from the Thymol Blue spectrum. The Thymol Blue spectral changes were measured at 590 or 650 nm, respectively, for dilute (<0.1 mM) or concentrated (>0.1 mM) Thymol Blue.

The stopped-flow traces shown in Figure 2 are representative progress curves comparing the azoaldehyde and Thymol Blue optical density changes observed under conditions where the extent of reaction is limited to a single turnover of those enzyme sites that encounter substrate (*e.g.*, when [NADH] > [E] > [aldehyde]). Under these single-turnover conditions, the disappearance of azoaldehyde (Figure 2, traces A and B) is a two-step process. The two steps (Bernhard *et al.*, 1970) have a greater than 10-fold difference in apparent first-order specific rate constants. The optical density change in each step accounts for approximately one-half of the total optical density change. Bernhard *et al.* (1970) have shown that each step corresponds to the conversion of aldehyde to alcohol[2] and NADH to NAD$^+$.

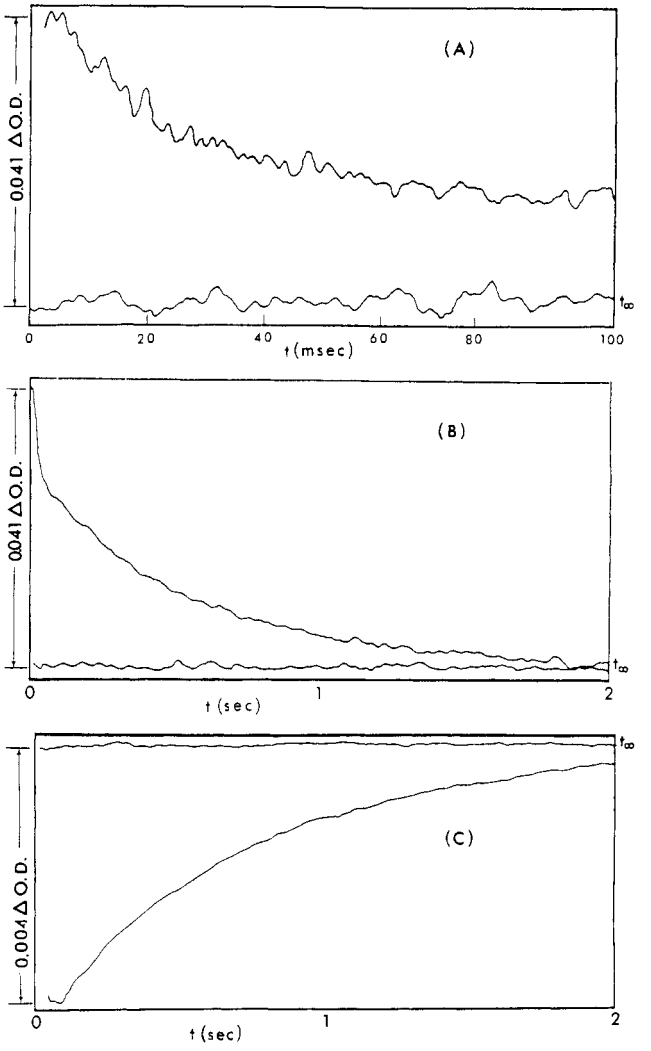

FIGURE 2: Representative stopped-flow traces comparing the time course for the disappearance of azoaldehyde at 390 nm, traces A and B, with the time course for the uptake of hydrogen ions as measured by the Thymol Blue spectral changes at 650 nm, trace C. Conditions: E, 12.5 μN; NADH, 78.8 μM; azoaldehyde, 5.60 μM; Thymol Blue, 49.5 μM; pH 8.8 ± 0.1 and 25.0 ± 0.2°. Note that the final optical density value corresponding to t_∞ is indicated for each time course, and that the optical density scale is corrected to that expected for a 1-cm light path.

In contrast to the biphasic time course observed at 390 nm, note that the Thymol Blue optical density changes (as shown in Figure 2, trace C) occur *via* a single (first-order) process. Furthermore, note that within the limits of experimental error, the apparent first-order specific rate constant for this process (Table I) is identical with the rate of the slow 390-nm step. The net Thymol Blue optical density change varies with the total Thymol Blue concentration, initially increasing and then approaching saturation at Thymol Blue concentrations >0.2 mM (Figure 3). By inspection of Figure 3, the saturated optical density change is estimated to be 0.016 ± 0.004 OD. This change corresponds to an estimated net change in the concen-

[2] The time course shown in Figure 2, traces A and B, is not unique to the azoaldehyde system. A number of aromatic substrates have been shown to behave in a completely analogous fashion (Bernhard *et al.*, 1970; Dunn and Bernhard, 1971; Luisi and Favilla, 1972), however, 4-*N*,*N*-dimethylaminocinnamaldehyde is a notable exception (Dunn and Hutchison, 1973).

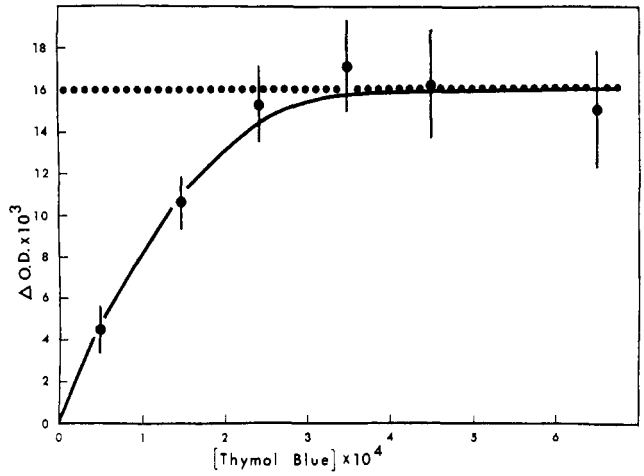

FIGURE 3: Dependence of the net Thymol Blue optical density change accompanying azoaldehyde reduction as a function of the total Thymol Blue concentration. Conditions: E, 12.5 μN; NADH, 78.8 μM; azoaldehyde, 5.60 μM; pH 8.8 ± 0.1 and 25.0 ± 0.2°.

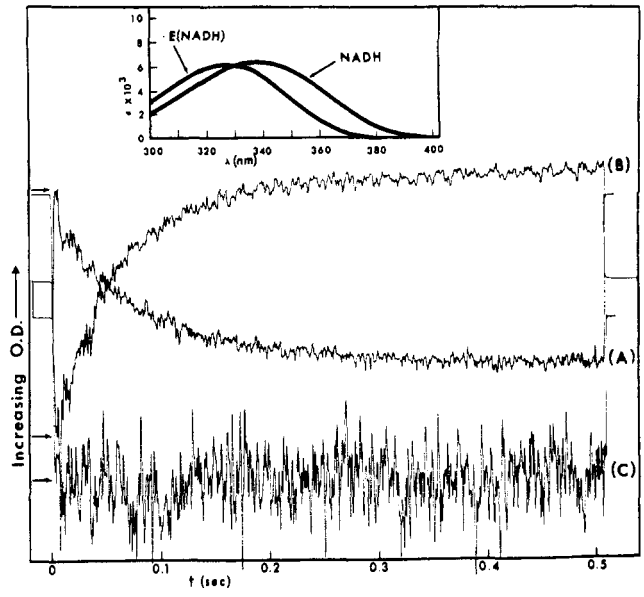

FIGURE 4: Representative stopped-flow traces comparing the time course for the formation of the enzyme–NADH binary complex measured at 365 nm (trace A) with the time course for the uptake of hydrogen ions as measured by the Thymol Blue spectral changes at 650 nm (trace B). Trace C measures the optical density at 330 nm, the isosbestic point for the two NADH species: enzyme bound and free in solution, see insert to this figure. Traces A and C were measured in 0.5 mM sodium pyrophosphate buffer (pH 8.80 ± 0.1). In trace B, 0.65 mM Thymol Blue, pH 8.8 ± 0.1, is the dominate buffer ion present in solution. Conditions: E, 10.6 μN; NAD^+, 23.9 μM; NADH, 94.1 μM; Thymol Blue, 0.384 mM; pH 8.8 ± 0.1 and 25.0 ± 0.2°. The net optical density changes (corrected to the values expected for a 1-cm light path) at 365 and 650 nm are 0.0120 and 0.0125 optical density, respectively. The insert to this figure compares the spectrum of NADH free in solution with the spectrum of enzyme-bound NADH.

tration of Thymol Blue chromophore of 5.5 ± 1 μM (calculated as $\Delta OD/\epsilon_{650}$ after correction for the enzyme–NADH buffering capacity, see Experimental Section). Equation 1 predicts a theoretical value of $[H^+] = 5.60$ μM for the total conversion of the limiting amount of azoaldehyde.

In order to verify the assumption that Thymol Blue acts only as a pH indicator and as the dominant buffer ion in this system, both steady-state kinetic studies and uv-visible spectral investigations of the system have been carried out. These investigations showed that Thymol Blue does not inhibit alcohol dehydrogenase, and no evidence for the formation of binary or ternary complexes between Thymol Blue and the other components of the system was found under the conditions employed in the stopped-flow experiments. In this context it should be noted that the presence of 1 mM pyrophosphate buffer completely eliminates the Thymol Blue spectral changes.

NAD^+ Displacement Studies. The spectrum of the alcohol dehydrogenase–NADH binary complex ($\lambda_{max} \simeq 327$ nm) is blue shifted by 13 nm relative to the 340-nm transition characteristic of NADH in neutral aqueous milieu (Theorell and Bonnichsen, 1951). The difference spectrum for NADH free in solution *vis á vis* the binary E(NADH) complex exhibits a broad minimum between 340 and 370 nm, and an isosbestic point at approximately 330 nm.

Together, these properties of the system make possible kinetic investigation of the enzyme–NAD^+ binary complex dissociation equilibria by monitoring the NADH spectral changes with the stopped-flow apparatus as the more affine enzyme–NADH complex is formed *via* displacement of bound NAD^+ by NADH (M. F. Dunn, J. T. McFarland, and S. A. Bernhard, unpublished work).

In the alkaline pH range, the rate of NAD^+ dissociation (k_1, eq 2) is known to be slow relative to the formation rate

$$\underset{\text{(binary complex)}}{E(NAD^+)} \underset{k_{-1}}{\overset{k_1}{\rightleftharpoons}} E + NAD^+ \qquad (2)$$

(k_2, eq 3) for the corresponding enzyme–NADH binary com-

$$E + NADH_{xs} \underset{k_{-2}}{\overset{k_2}{\rightleftharpoons}} \underset{\text{(binary complex)}}{E(NADH)} \qquad (3)$$

plex (Theorell and Chance, 1951; Geraci and Gibson, 1967). At pH 8.8, the specific first-order rate constant for NAD^+ dissociation, k_1, is 10–15 sec^{-1} (Theorell and Chance, 1951; S. A. Bernhard, J. T. McFarland, and M. F. Dunn, unpublished work). Therefore, on mixing solutions of NADH with solutions containing the enzyme–NAD^+ complex, the rate of NAD^+ dissociation will limit the rate of interchange of NADH

TABLE 1: A Comparison of the Apparent First-Order Rate Constants for Azoaldehyde Reduction,[a] k_{390}, and Hydrogen Ion Uptake, k_{650}, as a Function of the pH Indicator (Thymol Blue) Concentration at pH 8.8 ± 0.1 and 25.0 ± 0.2.

[Thymol Blue] (mM)	k_{390} (sec^{-1})[c]	k_{650} (sec^{-1})[c]
0	1.65 ± 0.2[b]	
0.0494	1.44 ± 0.3	1.49 ± 0.2
0.121	1.55 ± 0.3	1.69 ± 0.2
0.190	1.68 ± 0.3	1.55 ± 0.2
0.237		1.75 ± 0.2
0.347		1.62 ± 0.2
0.453		1.44 ± 0.2
0.650		1.49 ± 0.2

[a] Conditions of concentration: E, 12.5 μN; NADH, 78.8 μM; S, 5.60 μM. [b] Measured in 0.1 M sodium pyrophosphate buffer (pH 8.75). [c] The apparent first-order rate constants, k_{390} and k_{650}, refer respectively to the rate of disappearance of the azoaldehyde measured at 390 nm (the slow step) and the rate of the acid–base mediated Thymol Blue spectral changes measured at 650 nm.

for bound NAD^+ since the magnitude of k_2 ($k_2 = 10^6$–10^7 M^{-1} sec^{-1}, Geraci and Gibson, 1967) ensures that the approach to equilibrium in eq 3 is relatively rapid for the conditions used in these experiments. Accordingly, the observable 365-nm optical density changes (Figure 4, trace A) reflect the apparent rate of NAD^+ desorption from the enzyme complex.

The addition of Thymol Blue to this system as buffer and pH indicator (just as previously discussed) provides a means for detecting any significant change in hydrogen ion concentration during the exchange reaction. Since the spectrum of NADH and the spectrum of Thymol Blue overlap extensively in the 300- to 390-nm region, the 365-nm NADH changes, and the 590- or 650-nm Thymol Blue changes have been examined in separate experiments (see Experimental Section).

A typical progress curve for the displacement of bound NAD^+ by NADH in dilute pyrophosphate buffer, as measured by the red shift in the spectrum of NADH on complex formation, is shown in Figure 4, trace A. That coenzyme exchange is the only reaction occurring on this time scale is demonstrated by the invariance of optical density (trace C) at the isosbestic point (330 nm) for the two NADH species (free and enzyme bound) in solution.[3]

For comparison, the progress curve (Figure 4, trace B) for the 650-nm optical density change is included, using solutions made up from the identical stocks of enzyme, NAD^+ and NADH, but employing Thymol Blue as indicator and buffer ion (see Experimental Section). The calculated first-order rate constants for these two processes are identical within the limits of experimental error (*e.g.*, 13.5 ± 1 and 12.6 ± 1 sec^{-1}, respectively). A twofold increase in the concentration of NADH over that employed in Figure 4 does not change the observed rate of change at either 365 or 650 nm.

The apparent stoichiometry ratio for the net moles of hydrogen ions consumed to the moles of NAD^+ displaced is estimated to be $\sim 1:1$ from the following calculations: The change in Thymol Blue anion concentration (Figure 4, trace B), corrected for the hydrogen ion change masked by the protein buffering capacity, measures the net hydrogen ion concentration change according to the relationship

$$\Delta[H^+] = \Delta[\text{Thymol Blue}](1/R) = (\Delta OD_{650}/\epsilon_{650})(1/0.85) \simeq 4.4 \pm 0.6\ \mu M \quad (4)$$

where R is the relative buffering capacity of Thymol Blue (see Experimental Section). The amount of enzyme–NADH binary complex formed, as determined by the total optical density change at 365 nm (Figure 4, trace A), is equal to the amount of NAD^+ displaced, thus

$$\Delta[\text{E–NAD}^+] = \Delta[\text{E–NADH}] = \Delta OD_{365}/\Delta\epsilon_{365} = 4.6 \pm 0.6\ \mu M \quad (5)$$

and

$$\Delta[H^+]/\Delta[\text{E–NAD}^+] = (4.4 \pm 0.6\ \mu M)/(4.6 \pm 0.6\ \mu M) = 0.91 \pm 0.3 \quad (6)$$

Discussion and Conclusions

The finding that the exchange of enzyme-bound NAD^+ for NADH results in a net uptake of hydrogen ions from solution is most reasonably explained as resulting from a shift in the pK_a' of a coenzyme-perturbed enzyme-site residue. Indeed, the coenzyme mediated perturbation of the pK_a' of a site residue could be predicted from the remarkable differences in the pH dependencies of the apparent, binary complex dissociation constants for enzyme-bound NAD^+ and for enzyme-bound NADH (Theorell and McKinley-McKee, 1961; Theorell and Winer, 1959; Dalziel, 1963; Taniguchi *et al.*, 1967; Iweido and Weiner, 1972; Coleman *et al.*, 1972). Shore *et al.* (1973) recently have shown that 1 equiv of protons is released at alkaline pH values when saturating amounts of NAD^+ are added to the enzyme.

Assuming the validity of this interpretation, then the lowering of the intrinsic pK_a' of this group in the enzyme–NAD^+ complex most likely is due to a strong Coulombic interaction between the positively charged nicotinamide moiety of NAD^+ when placed in close proximity to the ionizable group within the binary complex. Such a pK_a' perturbation has ample chemical precedent, *viz.*, the "perturbed" pK_a''s exhibited by the amino acids in comparison to their normal aliphatic carboxylic acid or aliphatic amine analogs; and such pK_a' perturbations have been previously identified for other protein systems (Parsons and Raftery, 1972; Oppenheimer *et al.*, 1966; Bernhard *et al.*, 1966; Hinz *et al.*, 1971).

The time course for azoaldehyde reduction under single-turnover conditions reflects a kinetic sequence of two steps; a "burst" reaction and a slow step. Bernhard *et al.* (1970) have previously shown that the spectral changes for the two-step sequence correspond to the formation of the azoalcohol and NAD^+ in each step. Furthermore, it has been shown that the products of the burst reaction dissociate from the enzyme site at a rate which can be no greater than the rate of the slow step (Bernhard *et al.*, 1970; Dunn and Bernhard, 1971; McFarland and Bernhard, 1972).

The present study shows that no net change in hydrogen ion concentration accompanies the burst reaction, even though a net transformation of substrate to product has occurred. The full change in hydrogen ion concentration predicted by eq 1 occurs at the rate of the slow second step (Figure 2). The above documented coenzyme-mediated change in the pK_a' of a site residue provides a simple explanation for this apparent paradox. For if the decrease in the pK_a' of the site residue is concomitant with the formation of NAD^+ in the burst, then the burst formation of NAD^+ will cause a burst release of an equivalent of hydrogen ions from the site. Therefore, the protons liberated by the pK_a' shift balance the proton uptake required to satisfy the chemical transformation, and so long as the enzyme site is occupied by NAD^+, there can be no net uptake of hydrogen ions from solution in this single-turnover experiment. Thus, the observed change in hydrogen concentration (Figure 2) is a consequence of the displacement of products from the enzyme sites by the large excess of NADH employed in these experiments.

Since both proton uptake and the slow step occur at identical rates, it is reasonable to conclude that both are limited by a common, rate-determining process. Previous studies (Bernhard *et al.*, 1970; Dunn and Bernhard, 1971; McFarland and Bernhard, 1972) have shown that the slow step is limited by the rate of product (alcohol) dissociation from the site. Because the rate of the slow step for the azoaldehyde system is significantly slower than the rate of NAD^+ dissociation from the enzyme–NAD^+ binary complex (1.6 ± 0.2 *vs.* 12.6 ± 1 sec^{-1}), the rate of NAD^+ desorption also appears to be limited by the same process which limits both the rate of proton uptake and the rate of the slow step.

Bernhard and McFarland (1972) also have shown that the burst process, but not the slow step, is subject to a primary

[3] Under the conditions of concentration employed in these experiments, the rate of combination of NADH with the fraction of free enzyme in solution on mixing occurs within the mixing dead time, and thus is not observed in these progress curves.

deuterium kinetic isotope effect ($k_H/k_D \simeq 2$) when stereospecifically labeled α-4-deuterio-NADH is compared to isotopically normal coenzyme. Thus, it is clear that, although the two steps each involve the same chemical transformation, the rate of each step is limited by a fundamentally different process. The burst process is rate limited by a step involving hydrogen transfer between NADH and azoaldehyde (*viz.* the kinetic isotope effect), and the slow step very probably is rate limited by a ligand dissociation process.

The results of the present study suggest a mechanism for the two-step transformation involving the concomitant isomerization of the active enzyme complex to an inactive conformation state in the burst step. It is possible that this isomerization is triggered by the perturbation of the pK_a' of a site residue (and the dissociation of a proton from the site) when NADH is converted to NAD^+ in the burst. If the active enzyme species is the fully liganded, $E(NADH,S)_2$ complex (as previously argued, Bernhard *et al.*, 1970; Dunn and Bernhard, 1971), then this mechanism predicts a "half-of-sites" burst reaction if the isomerization occurs at a rate which is greater than the rate of the burst.

According to this proposal, the active conformation is regained in the slow step at a rate which, in the case of the azoaldehyde system, is limited by the rate of dissociation of products.

References

Bates, R. G. (1964), Determination of pH; Theory and Practice, Wiley, New York, N. Y., p 435.

Bernhard, S. A., Dunn, M. F., Luisi, P. L., and Schack, P. (1970), *Biochemistry 9*, 185.

Bernhard, S. A., Hershberger, E., and Keiser, J. (1966), *Biochemistry 5*, 4120.

Brändén, C.-I., Eklund, H., Nordström, B., Boiwe, T., Söderlund, G., Zeppezauer, E., Ohlsson, I., and Åkeson, Å. (1973), *Proc. Nat. Acad. Sci. U. S. 70*, 2439.

Coleman, P. L., Iweibo, I., and Weiner, H. (1972), *Biochemistry 11*, 1010.

Dalziel, K. (1957), *Acta Chem. Scand. 11*, 396.

Dalziel, K. (1963), *J. Biol. Chem. 230*, 2850.

Dunn, M. F., and Bernhard, S. A. (1971), *Biochemistry 10*, 4569.

Dunn, M. F., and Hutchison, J. S. (1973), *Biochemistry 12*, 4882.

Everse, J. (1973), *Mol. Pharmacol. 9*, 199.

Geraci, G., and Gibson, Q. H. (1967), *J. Biol. Chem. 242*, 4275.

Hinz, H. J., Shiao, D. D. F., and Sturtevant, J. M. (1971), *Biochemistry 10*, 1347.

Iweibo, I., and Weiner, H. (1972), *Biochemistry 11*, 1003.

Jörnvall, H. (1973), *Proc. Nat. Acad. Sci. U. S. 70*, 2295.

Keiser, J., and Bernhard, S. A. (1966), *Biochemistry 5*, 4127.

Luisi, P. L., and Favilla, R. (1972), *Biochemistry 11*, 2303.

McFarland, J. T., and Bernhard, S. A. (1972), *Biochemistry 11*, 1486.

Oppenheimer, H. L., Labouesse, B., and Hess, G. P. (1966), *J. Biol. Chem. 241*, 2720.

Parsons, S. M., and Raftery, M. A. (1972), *Biochemistry 11*, 1623, 1630, 1633.

Shore, J. D., Gutfreund, H., Santiago, D., and Santiago, P. (1973), *1st Intern. Symp. Alcohol Aldehyde Metabol. Systems, Stockholm*, July 9–11.

Sund, H., and Theorell, H. (1962), *Enzymes 7*, 26.

Taniguchi, S., Theorell, H., and Åkeson, Å. (1967), *Acta Chem. Scand. 21*, 1903.

Theorell, H., and Bonnichsen, R. (1951), *Acta Chem. Scand. 5*, 1105.

Theorell, H., and Chance, B. (1951), *Acta Chem. Scand. 15*, 1811.

Theorell, H., and McKinley-McKee, J. S. (1961), *Acta Chem. Scand. 15*, 1811.

Theorell, H., and Winer, A. D. (1959), *Arch. Biochem. Biophys. 83*, 291.

Theorell, H., and Yonetani, T. (1963), *Biochem. Z. 338*, 537.